

Performance of integrated optical switches based on 2D materials and beyond

Yuhan YAO, Zhao CHENG, Jianji DONG (✉), Xinliang ZHANG

Wuhan National Laboratory for Optoelectronics, Huazhong University of Science and Technology, Wuhan 430074, China

© Higher Education Press 2020

Abstract Applications of optical switches, such as signal routing and data-intensive computing, are critical in optical interconnects and optical computing. Integrated optical switches enabled by two-dimensional (2D) materials and beyond, such as graphene and black phosphorus, have demonstrated many advantages in terms of speed and energy consumption compared to their conventional silicon-based counterparts. Here we review the state-of-the-art of optical switches enabled by 2D materials and beyond and organize them into several tables. The performance tables and future projections show the frontiers of optical switches fabricated from 2D materials and beyond, providing researchers with an overview of this field and enabling them to identify existing challenges and predict promising research directions.

Keywords two-dimensional (2D) materials, integrated optics, optical switches, performance table

1 Introduction

Optical switches are increasingly considered for applications in optical computing and interconnections in order to meet the ever-growing performance demands in data centers [1,2]. With the advent of the Big Data era, Moore's Law is approaching its physical limit. Traditional photonic integrated circuits (PICs) face crucial challenges in energy consumption, operation speed, and fabrication cost. As the basic units of large-scale PICs, integrated optical switches are of great significance for use in interconnections, the performance of which always determines the upper limit of the whole circuit. To provide switches with greater applicability to high-performance optoelectronics, it is essential to design an optical switch with a small footprint, low energy consumption, and fast response time.

Conventional integrated optical switches utilize variations in the effective refractive index of the waveguide produced, including the thermo-optic effect [3–7] or plasma dispersion [8–10]. However, conventional switches have hit a technical limit imposed by the properties of traditional bulk materials, which cannot adequately satisfy the growing needs [11]. Consequently, investigators have developed hybrid structures to improve the performance of optical switches, using active substances, such as two-dimensional (2D) materials [12,13] and polymers [14,15], that are introduced into the traditional optical devices. In recent years, 2D materials, such as graphene, black phosphorus, and transition-metal dichalcogenides, have become increasingly attractive for integrated photonic applications in light sources, modulators, and photodetectors [16–21]. Their atomically thin structures reduce the dimensionality of the material, resulting in unique optical and electronic properties—including high electron mobility [22–25], strong anisotropy [26,27], strong photoluminescence [28,29], tunable bandgaps [30,31], large optical nonlinearity [32–36], etc.—that provide great opportunities for improving the performance of optoelectronic devices. In particular, the combination of 2D materials and complementary metal-oxide-semiconductor (CMOS)-compatible integrated photonics appears very promising. It can compensate for the intrinsic drawbacks of the waveguide itself [37], thus providing great potential for realizing high-performance optical switches. Note that all the optical switches mentioned below refer particularly to devices integrated with 2D materials and beyond.

In communication systems, the properties of switches, such as the extinction ratio, insertion loss, and footprint, must be carefully considered. We specifically focus on the operation speed and energy consumption because these two parameters are of most concern for realistic applications in large-scale PICs. Furthermore, we expect that future interconnect technologies will demand optical components on a chip that consume less energy than one femtojoule per bit [38]. In particular, we present complete

tables containing representative optical switches, providing a useful information resource that summarizes the work in this area. In addition, the performance of various optical switches is summarized in terms of switching time and energy consumption. These data will be updated with further progress in this field to provide more support for investigators.

2 Criterion for statistics

The optical switches discussed in this article refer to time-domain switches or optical modulators rather than to spatial switches or optical routers that use $N \times N$ optical-switch fabric, which can be built up by connecting the basic switching cells into switching-fabric topologies [39–47]. In addition, noteworthy results in mode-multiplexed photonic switches are not included [48–51], as we focus exclusively on single-mode systems. All the data in the following tables and figures are taken from studies published before April 2020. Different physical mecha-

nisms have been explored to trigger the optical switching process in integrated devices, which can be classified into all-optical, thermo-optical, and electro-optical switching. Energy consumption in integrated devices is always used to rank the switching performance [38]. To allow for a detailed and comprehensive analysis, we chose different units to evaluate the energy consumption for each type of mechanism. We selected energy per bit (E/bit) for all-optical and electro-optical switching and selected the minimum power per free spectral range (FSR) (mW/FSR) for thermo-optical switching.

3 Performance tables

Table 1 lists the representative studies of all-optical switches over the years. Most are 2D materials-based hybrid structures, although a few are polymer-based devices. The columns include the switching principle, material, device structure, energy consumption, switching time, and publication date. Table 2 lists several excellent

Table 1 Performance list of all-optical switches with energy consumption and switching time

switching principle	material	device structure	energy consumption (fJ·bit ⁻¹)	switching time /ps	publication time	Ref.
carrier-induced nonlinearity	InGaAsP	PhC nanocavity	0.66	35	May. 2010	[53]
carrier-induced nonlinearity	InGaAsP	PhC nanocavity	2.5	44	Feb. 2012	[54]
saturable absorption	graphene	plasmonic waveguide	35	0.26	Nov. 2019	[55]
optical nonlinearity	polymer	photonic-bandgap microcavity	520	1.2	Feb. 2008	[56]
third-order nonlinearity	WSe ₂	metallic waveguide	650	0.29	Jul. 2019	[57]
saturable absorption	graphene	straight waveguide	2100	1.65	Mar. 2020	[58]
carrier-induced nonlinearity	CdS	free-standing nanowires /silicon waveguides	NA	NA	Jun. 2017	[59]
photoluminescence	WS ₂	straight waveguide	NA	NA	Nov. 2017	[60]

Notes: NA—not available, PhC—photonic crystal.

Table 2 Performance list of thermo-optical switches with tuning efficiency and rise/decay times

switching principle	device structure	tuning efficiency/(mW·FSR ⁻¹)	rise/decay times/μs	publication time	Ref.
graphene microheaters	silicon PhC waveguides	3.99	0.75/0.525	Feb. 2017	[61]
graphene heater	silicon MZI	6.6	980/520	Mar. 2020	[62]
black arsenic-phosphorus micro-heater	silicon MZI	9.48	30/20	Jan. 2020	[63]
thermal-optic effect of black phosphorus	silicon MRR	12.2	0.479/0.113	Jan. 2020	[64]
graphene nanoheaters	silicon microdisk resonator	47.25	12.8/8.8	Feb. 2016	[65]
graphene heat conductor	silicon MZI	141	20/20	Dec. 2014	[66]
thermal conductivity of graphene	Si ₃ N ₄ MRR	683.5	0.253/0.888	Dec. 2017	[67]
graphene heater	silicon MRR	NA	0.75/0.8	Oct. 2015	[68]
graphene microheater	silicon nanobeam cavity	1.5 nm/mW	1.11/1.47	Aug. 2017	[69]

Notes: NA—not available, PhC—photonic crystal, MZI—Mach-Zehnder interferometer, MRR—microring resonator. The phase change is calculated as $\Delta\phi = \frac{\Delta\lambda}{\text{FSR}}2\pi$.

thermo-optical switches. Here the 2D materials work as heat conductors or transparent heaters. Table 3 lists the best-performing electro-optical switches, which are the most studied and the closest to practical industrial applications, with the best power consumption of 0.7 fJ/bit [52].

The following charts track the progress and trends of the switching energy and switching time. Figure 1(a) shows the trend in energy consumption of all-optical and electro-optical switches in recent years. The overall energy consumption of all-optical switches based on 2D materials is 1–3 orders of magnitude lower than that of electro-optical switches, the performance of which fluctuates slightly around hundreds of femtojoules. Notably, the switching energy of optical switches with plasmonic-graphene hybrid waveguides can be reduced significantly, to 35 fJ/bit [55]. This suggests a new solution for energy-efficient processing, which is further discussed in the next section. Figure 1(b) depicts the tuning efficiency of thermo-optic switches over time. By incorporating monolayer graphene with a silicon photonic-crystal waveguide, a graphene microheater has the lowest reported power consumption (3.99 mW per FSR), which is attributed to the slow-light waveguide greatly enhancing the light-matter interactions.

Figure 2 presents the trend in switching time of all-optical, thermo-optical, and electro-optical switches over time. Overall, the speed of all three mechanisms has dropped by almost two orders of magnitude over the past

10 years. All-optical switching has the fastest switching time (sub-picosecond level), since it can be completely implemented in the optical domain, avoiding the conversion from external electronic signals to optical ones. Thermo-optical switches typically employ heating to change the phase of the light beam. Graphene, used as a transparent heater, has been integrated onto various silicon photonic-crystal waveguides to provide enhanced tuning efficiency, and it outperforms conventional metallic microheaters [61,69]. Unfortunately, the response times are relatively slow (hundreds of nanoseconds to tens of microseconds) because of the intrinsically slow thermal diffusivity. In contrast, the device response of electro-optical switches is limited by the electrical bandwidth rather than by the intrinsic speed of the material. Since graphene has an ultrahigh electron mobility [23], the modulation speed is consequently limited by the RC time constant of the modulator, which can be enhanced with structural optimization of the electro-optical modulators [71,74,76,78,79].

Next, we further subdivide optical switches into categories according to the different device structures. Figure 3 shows the performance of various switching devices in two dimensions (energy and time) simultaneously. For all-optical switches (Fig. 3(a)), photonic-crystal microcavities and plasmonic waveguides show obvious advantages on the energy-time-product line compared to conventional waveguides. For thermo-optic switches (Fig. 3(b)), Mach–Zehnder interferometer (MZI)

Table 3 Performance list of electro-optical switches with energy consumption and operation speed

switching principle	material	device structure	energy consumption /(fJ·bit ⁻¹)	operation speed /GHz	publication time	Ref.
Pockels effect	polymer	silicon slot waveguide	0.7	NA	Feb. 2015	[52]
electro-optic effect	polymer	plasmonic slot waveguide	25	70	Jul. 2015	[70]
electrically tuning	graphene/graphene capacitor	silicon PhC waveguide	275	12	Nov. 2019	[71]
electrically gating	graphene	air-slot PhC nanocavity	340	NA	Jan. 2013	[72]
electrically tuning	graphene	silicon rib waveguide	350	2.6–5.9	Jan. 2016	[73]
electrically tuning	graphene/graphene capacitor	silicon nitride MRR	800	30	Jul. 2015	[74]
gate tuning Fermi level	graphene	silicon MRR	900	NA	Nov. 2014	[75]
electrically tuning Fermi level	double-layer graphene	silicon waveguide	1000	1	Feb. 2012	[76]
electrically gating	graphene-boron nitride heterostructure	silicon PhC nanocavity	1000	1.2	Feb. 2015	[77]
electrically tuning	graphene	silicon MZI	1000	5	Dec. 2017	[78]
electrically gating	graphene/graphene capacitor	silicon straight waveguide	1400	35	Sep. 2016	[79]
Pockels effect	polymer	silicon slot waveguide	NA	100	May. 2014	[80]
electrically tuning Fermi level	graphene	silicon bus waveguide	NA	1.2	May. 2011	[81]

Notes: PhC—photonic crystal, MRR—microring resonator, MZI—Mach–Zehnder interferometer, NA—not available. The energy per bit (E/bit) is calculated as $E/\text{bit} = 1/4CV^2$, where C is the device capacitance and V is the driving voltage [82].

type optical switches are all located on a roughly similar energy-time-product line, but the photonic-crystal waveguides and optimized microring resonators are located away from this line. For electro-optical switches (Fig. 3(c)), plasmonic waveguides show significant advantages.

4 What lies behind the statistics

4.1 Pros and cons of the three different mechanisms

As mentioned above, optical switches can be classified into all-optical, thermo-optical, and electro-optical switches, according to the switching mechanism. All-optical switches are the most promising candidates for use in PICs because of their energy-efficient power consumption and high-speed switching times, since they avoid electro-optical conversion. All-optical switches use the nonlinear properties of the material to control one light beam by another. The key to reducing energy consumption without affecting speed is effectively to enhance the nonlinear interaction in a limited volume. This can be achieved by using high-quality microring resonators, photonic-crystal microcavities, and metallic nanostructures. An all-optical switch with a graphene-loaded plasmonic waveguide shows superior performance, with an ultralow switching energy of 35 fJ/bit and an ultrafast switching time of 260 fs, thanks to the extremely strong light confinement in the plasmonic slot waveguide, which enhances the nonlinear absorption in graphene [55]. By using 2D materials as thermal conductors or transparent nanoheaters, thermo-optical switching can be achieved with a simple configuration having high efficiency, an easy fabrication process, and low cost. However, due to the slowness of thermal

diffusion itself, the fastest switching time is only in the hundreds of nanoseconds. An electro-optical switch is one based on the electro-optic effect, that is, on the change in the refractive index of the material caused by a direct current (DC) or an alternating current (AC) electric field. This effect can be obtained either from nonlinear optical materials or from linear electro-optic materials. Electro-optic switching is widely used in high-speed optical interconnections, due to its ability to connect the electrical domain with the optical domain. However, it often requires complex structural optimization, and the insertion loss is relatively high, which are challenges that remain to be improved in the future.

4.2 Results for different device structures

Figure 3 illustrates schematically that the overall performance of a device is affected by the different waveguide structures, such as a photonic-crystal waveguide, plasmonic waveguide, microring, and MZI. The MZI-type optical switches are among the most commonly used building blocks in PICs, and they have great advantages in the fabrication process, manufacturing cost, and good scalability. However, because they are non-resonant devices, they have been criticized for their lower energy efficiency and less compactness. Additional control of the powers obtained from the two arms of the interferometer is also required to maximize the extinction ratio [83]. Conversely, the resonance effect in an optical microcavity is capable of enhancing the light sensitivity. Photonic-crystal waveguides and microring resonators can significantly increase the light-matter interaction inside the switch. Therefore, resonant cavities with large quality-to-volume (Q/V) ratios are very promising candidates for reducing the energy consumption and shrinking the footprint of a device.

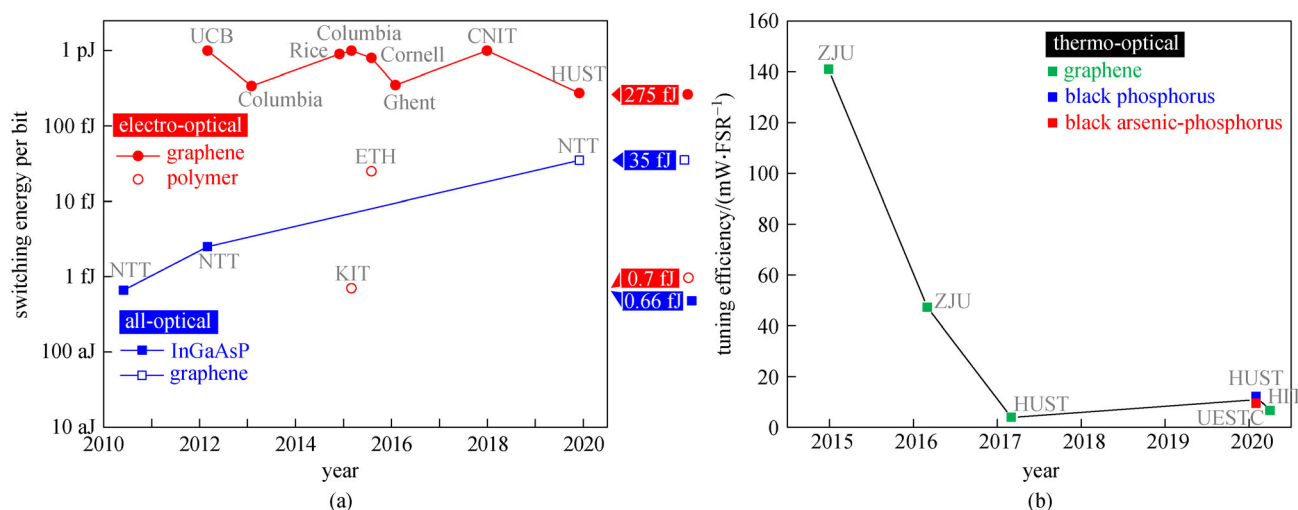


Fig. 1 (a) Trends in energy consumption of all-optical and electro-optical switches over time. (b) Trends in the energy consumption of thermo-optical switches over time

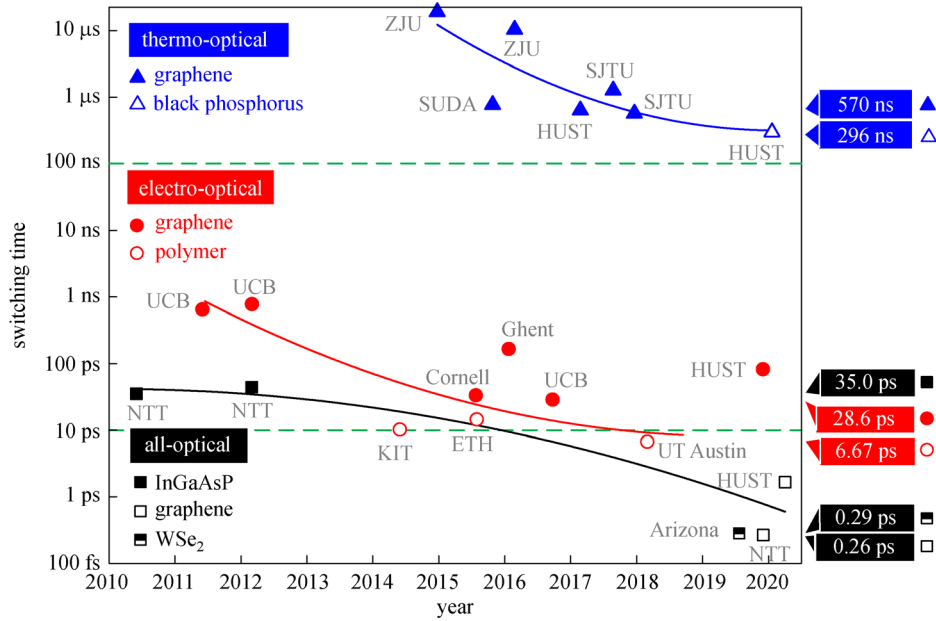


Fig. 2 Trends in the switching time of all-optical, electro-optical, and thermo-optical switches over time. The switching time is the average of the rise and decay times

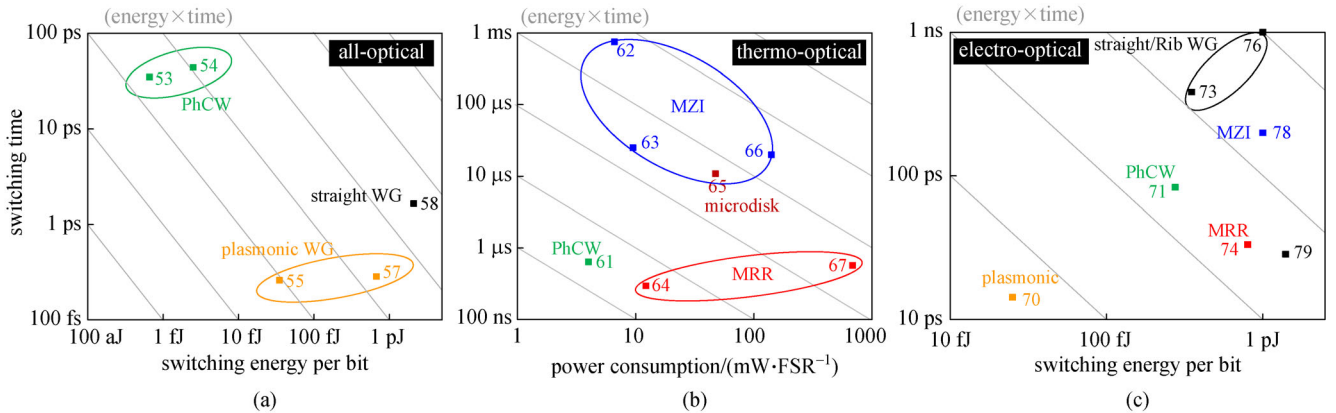


Fig. 3 (a) Performance of various all-optical switches. (b) Performance of various thermo-optical switches. (c) Performance of various electro-optical switches. The switching time and switching energy per bit/tuning efficiency are indicated for switches using a photonic-crystal waveguide (PhCW) [53,54,61,71], plasmonic waveguide (WG) [55,57,70], straight waveguide [58,76,79], rib waveguide [73], Mach-Zehnder interferometer (MZI) [62,63,66,78], microdisk [65], and microring resonator (MRR) [64,67,74]

However, the resonance effect is usually for light of a specific frequency, which limits the operating-wavelength range, and both thermal and fabrication tolerance remain challenges for practical use [84]. Combinations of nanomaterials with integrated plasmonic nanostructures are also being explored to provide an alternative way to enhance the light-matter interactions [85–89]. Metallic nanostructures that support surface plasmon polaritons show strong abilities to concentrate light within the subwavelength region, providing great potential for realizing high-performance optoelectronic devices with compact footprints [90].

4.3 Ultrafast integrated optical switches with ultralow switching energies remain an ongoing challenge

At present, the integration of 2D materials into photonic platforms is still limited. Although they are not very mature, 2D materials are far more accessible and flexible than their III-V counterparts [91–94], and they may prove to be more adaptable for on-chip integration using simple, cheap, and scalable post-processing techniques. In the rich family of 2D materials, more candidates are worth exploring, and the bottleneck in utilizing them for large-scale applications may soon be overtaken by recent

breakthroughs in wafer-scale, synthesis methods and manufacturing processes [95–97]. In the past few years, assisted by 2D materials and beyond, several breakthroughs have been made in integrated optical switches, in terms of switching time and energy consumption. However, it is still difficult to reduce the energy consumption further to the attojoule level, which is essential for future large-scale PICs. This requires meticulous, systematic, and deep exploration of the mechanism responsible for enhancing light-matter interactions, that is, of the interaction mechanisms and methods for controlling multi-physical (optical, thermal, electric) fields within the medium. Based on the performance of emerging nanomaterials and plasmonic, nanophotonic, hybrid integration performs, ultrafast switching with energy consumption at the attojoule level may be achievable [98]. More effort must be devoted to this field to improve the performance further.

Appendix

Table A1 Explanatory notes of the labels used in Figs. 1 and 2

label	full name
Arizona	University of Arizona
CNIT	Consorzio Nazionale per le Telecomunicazioni
Columbia	Columbia University
Cornell	Cornell University
ETH	ETH Zurich
Ghent	Ghent University
HIT	Harbin Institute of Technology
HUST	Huazhong University of Science and Technology
KIT	Karlsruhe Institute of Technology
NTT	NTT Basic Research Laboratories
Rice	Rice University
SJTU	Shanghai Jiao Tong University
SUDA	Soochow University
UCB	University of California at Berkeley
UESTC	University of Electronic Science and Technology
UT Austin	University of Texas at Austin
ZJU	Zhejiang University

Acknowledgements This work was supported in part by the National Key Research and Development Project of China (No. 2018YFB2201901) and in part by the National Natural Science Foundation of China (Grant No. 61805090).

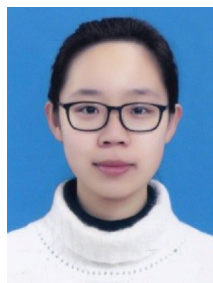
References

- Cheng Q, Bahadori M, Glick M, Rumley S, Bergman K. Recent advances in optical technologies for data centers: a review. *Optica*, 2018, 5(11): 1354
- Cheng Q, Rumley S, Bahadori M, Bergman K. Photonic switching in high performance datacenters. *Optics Express*, 2018, 26(12): 16022–16043
- Geis M W, Spector S J, Williamson R C, Lyszczarz T M. Submicrosecond submilliwatt silicon-on-insulator thermo-optic switch. *IEEE Photonics Technology Letters*, 2004, 16(11): 2514–2516
- Dong P, Qian W, Liang H, Shafiqi R, Feng D, Li G, Cunningham J E, Krishnamoorthy A V, Asghari M. Thermally tunable silicon racetrack resonators with ultralow tuning power. *Optics Express*, 2010, 18(19): 20298–20304
- Lee B S, Zhang M, Barbosa F A S, Miller S A, Mohanty A, St-Gelais R, Lipson M. On-chip thermo-optic tuning of suspended microresonators. *Optics Express*, 2017, 25(11): 12109–12120
- Li X, Xu H, Xiao X, Li Z, Yu Y, Yu J. Fast and efficient silicon thermo-optic switching based on reverse breakdown of pn junction. *Optics Letters*, 2014, 39(4): 751–753
- Zhao Y, Wang X, Gao D, Dong J, Zhang X. On-chip programmable pulse processor employing cascaded MZI-MRR structure. *Frontiers of Optoelectronics*, 2019, 12(2): 148–156
- Xu Q, Manipatruni S, Schmidt B, Shakya J, Lipson M. 12.5 Gbit/s carrier-injection-based silicon micro-ring silicon modulators. *Optics Express*, 2007, 15(2): 430–436
- Manipatruni S, Dokania R K, Schmidt B, Sherwood-Droz N, Poitras C B, Apsel A B, Lipson M. Wide temperature range operation of micrometer-scale silicon electro-optic modulators. *Optics Letters*, 2008, 33(19): 2185–2187
- Timurdogan E, Sorace-Agaskar C M, Sun J, Shah Hosseini E, Biberman A, Watts M R. An ultralow power athermal silicon modulator. *Nature Communications*, 2014, 5(1): 4008
- Ferrari A C, Bonaccorso F, Fal'ko V, Novoselov K S, Roche S, Bøggild P, Borini S, Koppens F H, Palermo V, Pugno N, Garrido J A, Sordan R, Bianco A, Ballerini L, Prato M, Lidorikis E, Kivioja J, Marinelli C, Ryhänen T, Morpurgo A, Coleman J N, Nicolosi V, Colombo L, Fert A, Garcia-Hernandez M, Bachtold A, Schneider G F, Guinea F, Dekker C, Barbone M, Sun Z, Galiotis C, Grigorenko A N, Konstantatos G, Kis A, Katsnelson M, Vandersypen L, Loiseau A, Morandi V, Neumaier D, Treossi E, Pellegrini V, Polini M, Tredicucci A, Williams G M, Hong B H, Ahn J H, Kim J M, Zirath H, van Wees B J, van der Zant H, Occhipinti L, Di Matteo A, Kinloch I A, Seyller T, Quesnel E, Feng X, Teo K, Rupasinghe N, Hakonen P, Neil S R, Tannock Q, Löfwander T, Kinaret J. Science and technology roadmap for graphene, related two-dimensional crystals, and hybrid systems. *Nanoscale*, 2015, 7(11): 4598–4810
- Xia F, Wang H, Xiao D, Dubey M, Ramasubramaniam A. Two-dimensional material nanophotonics. *Nature Photonics*, 2014, 8(12): 899–907
- Sun Z, Martinez A, Wang F. Optical modulators with 2D layered materials. *Nature Photonics*, 2016, 10(4): 227–238
- Koos C, Vorreau P, Vallaitis T, Dumon P, Bogaerts W, Baets R, Esembeson B, Biaggio I, Michinobu T, Diederich F, Freude W, Leuthold J. All-optical high-speed signal processing with silicon-organic hybrid slot waveguides. *Nature Photonics*, 2009, 3(4): 216–219
- Melikyan A, Alloatti L, Muslija A, Hillerkuss D, Schindler P C, Li J,

- Palmer R, Korn D, Muehlbrandt S, Van Thourhout D, Chen B, Dinu R, Sommer M, Koos C, Kohl M, Freude W, Leuthold J. High-speed plasmonic phase modulators. *Nature Photonics*, 2014, 8(3): 229–233
16. Mueller T, Xia F, Avouris P. Graphene photodetectors for high-speed optical communications. *Nature Photonics*, 2010, 4(5): 297–301
 17. Youngblood N, Chen C, Koester S J, Li M. Waveguide-integrated black phosphorus photodetector with high responsivity and low dark current. *Nature Photonics*, 2015, 9(4): 247–252
 18. Datta I, Chae S H, Bhatt G R, Tadayon M A, Li B, Yu Y, Park C, Park J, Cao L, Basov D N, Hone J, Lipson M. Low-loss composite photonic platform based on 2D semiconductor monolayers. *Nature Photonics*, 2020, 14(4): 256–262
 19. Wu S, Buckley S, Schaibley J R, Feng L, Yan J, Mandrus D G, Hatami F, Yao W, Vučković J, Majumdar A, Xu X. Monolayer semiconductor nanocavity lasers with ultralow thresholds. *Nature*, 2015, 520(7545): 69–72
 20. Ye Y, Wong Z J, Lu X, Ni X, Zhu H, Chen X, Wang Y, Zhang X. Monolayer excitonic laser. *Nature Photonics*, 2015, 9(11): 733–737
 21. Yao Y, Xia X, Cheng Z, Wei K, Jiang X, Dong J, Zhang H. All-optical modulator using MXene inkjet-printed microring resonator. *IEEE Journal of Selected Topics in Quantum Electronics*, 2020, doi:10.1109/JSTQE.2020.2982985
 22. Youngblood N, Li M. Integration of 2D materials on a silicon photonics platform for optoelectronics applications. *Nanophotonics*, 2016, 6(6): 1205–1218
 23. Bolotin K I, Sikes K J, Jiang Z, Klima M, Fudenberg G, Hone J, Kim P, Stormer H L. Ultrahigh electron mobility in suspended graphene. *Solid State Communications*, 2008, 146(9–10): 351–355
 24. Mas-Ballesté R, Gómez-Navarro C, Gómez-Herrero J, Zamora F. 2D materials: to graphene and beyond. *Nanoscale*, 2011, 3(1): 20–30
 25. Kang K, Xie S, Huang L, Han Y, Huang P Y, Mak K F, Kim C J, Muller D, Park J. High-mobility three-atom-thick semiconducting films with wafer-scale homogeneity. *Nature*, 2015, 520(7549): 656–660
 26. Tran V, Soklaski R, Liang Y, Yang L. Layer-controlled band gap and anisotropic excitons in few-layer black phosphorus. *Physical Review B*, 2014, 89(23): 235319
 27. Qiao J, Kong X, Hu Z X, Yang F, Ji W. High-mobility transport anisotropy and linear dichroism in few-layer black phosphorus. *Nature Communications*, 2014, 5(1): 4475
 28. Autere A, Jussila H, Dai Y, Wang Y, Lipsanen H, Sun Z. Nonlinear optics with 2D layered materials. *Advanced Materials*, 2018, 30(24): 1705963
 29. Li Y, Zhang J, Huang D, Sun H, Fan F, Feng J, Wang Z, Ning C Z. Room-temperature continuous-wave lasing from monolayer molybdenum ditelluride integrated with a silicon nanobeam cavity. *Nature Nanotechnology*, 2017, 12(10): 987–992
 30. Mak K F, Lee C, Hone J, Shan J, Heinz T F. Atomically thin MoS₂: a new direct-gap semiconductor. *Physical Review Letters*, 2010, 105(13): 136805
 31. Naguib M, Kurtoglu M, Presser V, Lu J, Niu J, Heon M, Hultman L, Gogotsi Y, Barsoum M W. Two-dimensional nanocrystals produced by exfoliation of Ti₃AlC₂. *Advanced Materials*, 2011, 23(37): 4248–4253
 32. Hendry E, Hale P J, Moger J, Savchenko A K, Mikhailov S A. Coherent nonlinear optical response of graphene. *Physical Review Letters*, 2010, 105(9): 097401
 33. Zhang H, Virally S, Bao Q, Ping L K, Massar S, Godbout N, Kockaert P. Z-scan measurement of the nonlinear refractive index of graphene. *Optics Letters*, 2012, 37(11): 1856–1858
 34. Jiang X, Liu S, Liang W, Luo S, He Z, Ge Y, Wang H, Cao R, Zhang F, Wen Q, Li J, Bao Q, Fan D, Zhang H. Broadband nonlinear photonics in few-layer MXene Ti₃C₂T_x (T = F, O, or OH). *Laser & Photonics Reviews*, 2018, 12(2): 1700229
 35. Jiang B, Hao Z, Ji Y, Hou Y, Yi R, Mao D, Gan X, Zhao J. High-efficiency second-order nonlinear processes in an optical microfiber assisted by few-layer GaSe. *Light, Science & Applications*, 2020, 9(1): 63
 36. Gu T, Petrone N, McMillan J F, van der Zande A, Yu M, Lo G Q, Kwong D L, Hone J, Wong C W. Regenerative oscillation and four-wave mixing in graphene optoelectronics. *Nature Photonics*, 2012, 6(8): 554–559
 37. Li J, Liu C, Chen H, Guo J, Zhang M, Dai D. Hybrid silicon photonic devices with two-dimensional materials. *Nanophotonics*, 2020, doi:10.1515/nanoph-2020-0093
 38. Miller D. Device requirements for optical interconnects to silicon chips. *Proceedings of the IEEE*, 2009, 97(7): 1166–1185
 39. Lu L, Zhao S, Zhou L, Li D, Li Z, Wang M, Li X, Chen J. 16 × 16 non-blocking silicon optical switch based on electro-optic Mach-Zehnder interferometers. *Optics Express*, 2016, 24(9): 9295–9307
 40. Jia H, Xia Y, Zhang L, Ding J, Fu X, Yang L. Four-port optical switch for fat-tree photonic network-on-chip. *Journal of Lightwave Technology*, 2017, 35(15): 3237–3241
 41. Lee B G, Dupuis N. Silicon photonic switch fabrics: technology and architecture. *Journal of Lightwave Technology*, 2019, 37(1): 6–20
 42. Jia H, Zhou T, Zhao Y, Xia Y, Dai J, Zhang L, Ding J, Fu X, Yang L. Six-port optical switch for cluster-mesh photonic network-on-chip. *Nanophotonics*, 2018, 7(5): 827–835
 43. Zheng D, Doménech J D, Pan W, Zou X, Yan L, Pérez D. Low-loss broadband 5 × 5 non-blocking Si₃N₄ optical switch matrix. *Optics Letters*, 2019, 44(11): 2629
 44. Li Z, Zhou L, Lu L, Zhao S, Li D, Chen J. 4 × 4 nonblocking optical switch fabric based on cascaded multimode interferometers. *Photonics Research*, 2016, 4(1): 21
 45. Seok T J, Quack N, Han S, Muller R S, Wu M C. Large-scale broadband digital silicon photonic switches with vertical adiabatic couplers. *Optica*, 2016, 3(1): 64
 46. Han S, Seok T J, Quack N, Yoo B W, Wu M C. Large-scale silicon photonic switches with movable directional couplers. *Optica*, 2015, 2(4): 370
 47. Sun J, Timurdogan E, Yaacobi A, Hosseini E S, Watts M R. Large-scale nanophotonic phased array. *Nature*, 2013, 493(7431): 195–199
 48. Yang L, Zhou T, Jia H, Yang S, Ding J, Fu X, Zhang L. General architectures for on-chip optical space and mode switching. *Optica*, 2018, 5(2): 180
 49. Xiong Y, Priti R B, Liboiron-Ladouceur O. High-speed two-mode switch for mode-division multiplexing optical networks. *Optica*, 2017, 4(9): 1098
 50. Jia H, Zhou T, Zhang L, Ding J, Fu X, Yang L. Optical switch

- compatible with wavelength division multiplexing and mode division multiplexing for photonic networks-on-chip. *Optics Express*, 2017, 25(17): 20698–20707
51. Zhou T, Jia H, Ding J, Zhang L, Fu X, Yang L. On-chip broadband silicon thermo-optic 2×2 four-mode optical switch for optical space and local mode switching. *Optics Express*, 2018, 26(7): 8375–8384
 52. Koeber S, Palmer R, Lauermann M, Heni W, Elder D L, Korn D, Woessner M, Alloatti L, Koenig S, Schindler P C, Yu H, Bogaerts W, Dalton L R, Freude W, Leuthold J, Koos C. Femtojoule electro-optic modulation using a silicon–organic hybrid device. *Light, Science & Applications*, 2015, 4(2): e255
 53. Nozaki K, Tanabe T, Shinya A, Matsuo S, Sato T, Taniyama H, Notomi M. Sub-femtojoule all-optical switching using a photonic-crystal nanocavity. *Nature Photonics*, 2010, 4(7): 477–483
 54. Nozaki K, Shinya A, Matsuo S, Suzuki Y, Segawa T, Sato T, Kawaguchi Y, Takahashi R, Notomi M. Ultralow-power all-optical RAM based on nanocavities. *Nature Photonics*, 2012, 6(4): 248–252
 55. Ono M, Hata M, Tsunekawa M, Nozaki K, Sumikura H, Chiba H, Notomi M. Ultrafast and energy-efficient all-optical switching with graphene-loaded deep-subwavelength plasmonic waveguides. *Nature Photonics*, 2020, 14(1): 37–43
 56. Hu X, Jiang P, Ding C, Yang H, Gong Q. Picosecond and low-power all-optical switching based on an organic photonic-bandgap microcavity. *Nature Photonics*, 2008, 2(3): 185–189
 57. Klein M, Badada B H, Binder R, Alfrey A, McKie M, Koehler M R, Mandrus D G, Taniguchi T, Watanabe K, LeRoy B J, Schaibley J R. 2D semiconductor nonlinear plasmonic modulators. *Nature Communications*, 2019, 10(1): 3264
 58. Wang H, Yang N, Chang L, Zhou C, Li S, Deng M, Li Z, Liu Q, Zhang C, Li Z, Wang Y. CMOS-compatible all-optical modulator based on the saturable absorption of graphene. *Photonics Research*, 2020, 8(4): 468
 59. Chen B, Wu H, Xin C, Dai D, Tong L. Flexible integration of free-standing nanowires into silicon photonics. *Nature Communications*, 2017, 8(1): 20
 60. Yang S, Liu D C, Tan Z L, Liu K, Zhu Z H, Qin S Q. CMOS-compatible WS_2 -based all-optical modulator. *ACS Photonics*, 2018, 5(2): 342–346
 61. Yan S, Zhu X, Frandsen L H, Xiao S, Mortensen N A, Dong J, Ding Y. Slow-light-enhanced energy efficiency for graphene microheaters on silicon photonic crystal waveguides. *Nature Communications*, 2017, 8(1): 14411
 62. Song Q Q, Chen K X, Hu Z F. Low-power broadband thermo-optic switch with weak polarization dependence using a segmented graphene heater. *Journal of Lightwave Technology*, 2020, 38(6): 1358–1364
 63. Liu Y, Wang H, Wang S, Wang Y, Wang Y, Guo Z, Xiao S, Yao Y, Song Q, Zhang H, Xu K. Highly efficient silicon photonic microheater based on black arsenic–phosphorus. *Advanced Optical Materials*, 2020, 8(6): 1901526
 64. Cheng Z, Cao R, Guo J, Yao Y, Wei K, Gao S, Wang Y, Dong J, Zhang H. Phosphorene-assisted silicon photonic modulator with fast response time. *Nanophotonics*, 2020, doi:10.1515/nanoph-2019-0510
 65. Yu L, Yin Y, Shi Y, Dai D, He S. Thermally tunable silicon photonic microdisk resonator with transparent graphene nanoheaters. *Optica*, 2016, 3(2): 159
 66. Yu L, Dai D, He S. Graphene-based transparent flexible heat conductor for thermally tuning nanophotonic integrated devices. *Applied Physics Letters*, 2014, 105(25): 251104
 67. Qiu C, Yang Y, Li C, Wang Y, Wu K, Chen J. All-optical control of light on a graphene-on-silicon nitride chip using thermo-optic effect. *Scientific Reports*, 2017, 7(1): 17046
 68. Gan S, Cheng C, Zhan Y, Huang B, Gan X, Li S, Lin S, Li X, Zhao J, Chen H, Bao Q. A highly efficient thermo-optic microring modulator assisted by graphene. *Nanoscale*, 2015, 7(47): 20249–20255
 69. Xu Z, Qiu C, Yang Y, Zhu Q, Jiang X, Zhang Y, Gao W, Su Y. Ultra-compact tunable silicon nanobeam cavity with an energy-efficient graphene micro-heater. *Optics Express*, 2017, 25(16): 19479–19486
 70. Haffner C, Heni W, Fedoryshyn Y, Niegemann J, Melikyan A, Elder D L, Baeuerle B, Salamin Y, Josten A, Koch U, Hoessbacher C, Ducry F, Juchli L, Emboras A, Hillerkuss D, Kohl M, Dalton L R, Hafner C, Leuthold J. All-plasmonic Mach–Zehnder modulator enabling optical high-speed communication at the microscale. *Nature Photonics*, 2015, 9(8): 525–528
 71. Cheng Z, Zhu X, Galili M, Frandsen L H, Hu H, Xiao S, Dong J, Ding Y, Oxenløwe L K, Zhang X. Double-layer graphene on photonic crystal waveguide electro-absorption modulator with 12 GHz bandwidth. *Nanophotonics*, 2019, doi:10.1515/nanoph-2019-0381
 72. Gan X, Shiue R J, Gao Y, Mak K F, Yao X, Li L, Szep A, Walker D Jr, Hone J, Heinz T F, Englund D. High-contrast electrooptic modulation of a photonic crystal nanocavity by electrical gating of graphene. *Nano Letters*, 2013, 13(2): 691–696
 73. Hu Y, Pantouvaki M, Van Campenhout J, Brems S, Asselberghs I, Huyghebaert C, Absil P, Van Thourhout D. Broadband 10 Gb/s operation of graphene electro-absorption modulator on silicon. *Laser & Photonics Reviews*, 2016, 10(2): 307–316
 74. Phare C T, Daniel Lee Y H, Cardenas J, Lipson M. Graphene electro-optic modulator with 30 GHz bandwidth. *Nature Photonics*, 2015, 9(8): 511–514
 75. Qiu C, Gao W, Vajtai R, Ajayan P M, Kono J, Xu Q. Efficient modulation of 1.55 μm radiation with gated graphene on a silicon microring resonator. *Nano Letters*, 2014, 14(12): 6811–6815
 76. Liu M, Yin X, Zhang X. Double-layer graphene optical modulator. *Nano Letters*, 2012, 12(3): 1482–1485
 77. Gao Y, Shiue R J, Gan X, Li L, Peng C, Meric I, Wang L, Szep A, Walker D Jr, Hone J, Englund D. High-speed electro-optic modulator integrated with graphene-boron nitride heterostructure and photonic crystal nanocavity. *Nano Letters*, 2015, 15(3): 2001–2005
 78. Soriano V, Midrio M, Contestabile G, Asselberghs I, Van Campenhout J, Huyghebaert C, Goykhman I, Ott A K, Ferrari A C, Romagnoli M. Graphene–silicon phase modulators with gigahertz bandwidth. *Nature Photonics*, 2018, 12(1): 40–44
 79. Dalir H, Xia Y, Wang Y, Zhang X. Athermal broadband graphene optical modulator with 35 GHz speed. *ACS Photonics*, 2016, 3(9): 1564–1568

80. Alloatti L, Palmer R, Diebold S, Pahl K P, Chen B, Dinu R, Fournier M, Fedeli J M, Zwick T, Freude W, Koos C, Leuthold J. 100 GHz silicon–organic hybrid modulator. *Light, Science & Applications*, 2014, 3(5): e173
81. Liu M, Yin X, Ulin-Avila E, Geng B, Zentgraf T, Ju L, Wang F, Zhang X. A graphene-based broadband optical modulator. *Nature*, 2011, 474(7349): 64–67
82. Miller D A B. Energy consumption in optical modulators for interconnects. *Optics Express*, 2012, 20(S2 Suppl 2): A293–A308
83. Qiao L, Tang W, Chu T. 32×32 silicon electro-optic switch with built-in monitors and balanced-status units. *Scientific Reports*, 2017, 7(1): 42306
84. Reed G T, Mashanovich G, Gardes F Y, Thomson D J. Silicon optical modulators. *Nature Photonics*, 2010, 4(8): 518–526
85. Yan S, Zhu X, Dong J, Ding Y, Xiao S. 2D materials integrated with metallic nanostructures: fundamentals and optoelectronic applications. *Nanophotonics*, 2020, doi:10.1515/nanoph-2020-0074
86. Ding Y, Guan X, Zhu X, Hu H, Bozhevolnyi S I, Oxenløwe L K, Jin K J, Mortensen N A, Xiao S. Efficient electro-optic modulation in low-loss graphene-plasmonic slot waveguides. *Nanoscale*, 2017, 9(40): 15576–15581
87. Ma P, Salamin Y, Baeuerle B, Josten A, Heni W, Emboras A, Leuthold J. Plasmonically enhanced graphene photodetector featuring 100 Gbit/s data reception, high responsivity, and compact size. *ACS Photonics*, 2019, 6(1): 154–161
88. Ding Y, Cheng Z, Zhu X, Yvind K, Dong J, Galili M, Hu H, Mortensen N A, Xiao S, Oxenløwe L K. Ultra-compact integrated graphene plasmonic photodetector with bandwidth above 110 GHz. *Nanophotonics*, 2020, 9(2): 317–325
89. Ansell D, Radko I P, Han Z, Rodriguez F J, Bozhevolnyi S I, Grigorenko A N. Hybrid graphene plasmonic waveguide modulators. *Nature Communications*, 2015, 6(1): 8846
90. Emboras A, Hoessbacher C, Haffner C, Heni W, Koch U, Ma P, Fedoryshyn Y, Niegemann J, Hafner C, Leuthold J. Electrically controlled plasmonic switches and modulators. *IEEE Journal of Selected Topics in Quantum Electronics*, 2015, 21(4): 276–283
91. Srinivasan S A, Pantouvaki M, Gupta S, Chen H T, Verheyen P, Lepage G, Roelkens G, Saraswat K, Thourhout D V, Absil P, Campenhout J V. 56 Gb/s germanium waveguide electro-absorption modulator. *Journal of Lightwave Technology*, 2016, 34(2): 419–424
92. Chen L, Dong P, Lipson M. High performance germanium photodetectors integrated on submicron silicon waveguides by low temperature wafer bonding. *Optics Express*, 2008, 16(15): 11513–11518
93. Liu J, Camacho-Aguilera R, Bessette J T, Sun X, Wang X, Cai Y, Kimerling L C, Michel J. Ge-on-Si optoelectronics. *Thin Solid Films*, 2012, 520(8): 3354–3360
94. Wang Z, Tian B, Pantouvaki M, Guo W, Absil P, Van Campenhout J, Merckling C, Van Thourhout D. Room-temperature InP distributed feedback laser array directly grown on silicon. *Nature Photonics*, 2015, 9(12): 837–842
95. Liu Y, Huang Y, Duan X. Van der Waals integration before and beyond two-dimensional materials. *Nature*, 2019, 567(7748): 323–333
96. Bae S H, Kum H, Kong W, Kim Y, Choi C, Lee B, Lin P, Park Y, Kim J. Integration of bulk materials with two-dimensional materials for physical coupling and applications. *Nature Materials*, 2019, 18(6): 550–560
97. Stanford M G, Rack P D, Jariwala D. Emerging nanofabrication and quantum confinement techniques for 2D materials beyond graphene. *npj 2D Materials and Applications*, 2018, 2(1): 20
98. Sorger V J, Amin R, Khurgin J B, Ma Z, Dalir H, Khan S. Scaling vectors of attoJoule per bit modulators. *Journal of Optics*, 2018, 20(1): 014012



Yuhan Yao is currently a Ph.D. candidate in Huazhong University of Science and Technology, Wuhan, China. Her current research interests include the integration of silicon photonics and two-dimensional materials as well as RF channelization.



Zhao Cheng is currently a Ph.D. candidate in Huazhong University of Science and Technology, Wuhan, China. His current research interests include 2D materials-based photonic modulators and photodetectors as well as photonic crystal waveguide.



Jianji Dong is a Professor at Wuhan National Laboratory for Optoelectronics, Huazhong University of Science and Technology (HUST), China. He received his Ph. D. degree of Optical Engineering from HUST in 2008. Subsequently, he worked as postdoc at Cambridge University, UK until 2010. From March 2010, he returned to HUST and was promoted to a full professor in 2013. His research interests include integrated microwave photonics, silicon photonics, and photonic computing. He has published more than 100 journal papers, including in *Nature Communications*, *Light Science and Applications*, and *Physical Review Letters*. He has made some special contributions to energy-efficient graphene silicon microheater, programmable temporal cloak, and complex spectrum analyzer of orbital angular momentum mode. He was honored with the Fund of Excellent Youth Scholar by the National Natural Science Foundation of China and honored with the First Award of Natural Science of Hubei Province. He is the editorial member of *Scientific Reports*, associate editor of *IET Optoelectronics*, and executive editor-in-chief of *Frontier of Optoelectronics*. He is an IEEE Senior Member and OSA member.



Xinliang Zhang received his Ph.D. degree in Physical Electronics from Huazhong University of Science and Technology (HUST), Wuhan, China in 2001. He is currently with Wuhan National Laboratory for Optoelectronics and School of Optical and Electronic Information, HUST as a Professor. He is the author or coauthor of more than 300 journal and conference papers. His current research interests include InP-based and Si-based devices and integration for optical network, high-performance computing and microwave photonics. In 2016, he was elected as an OSA Fellow.